Proceedings of ERAD (2002): 104–112 © Copernicus GmbH 2002

ERAD 2002

# Influence of disdrometer deadtime correction on self-consistent analytical parameterizations for raindrop size distributions

**R. Uijlenhoet**[1], **M. Steiner**[2], **and J. A. Smith**[2]

[1]Hydrology and Quantitative Water Management Group, Department of Environmental Sciences, Wageningen University, The Netherlands

[2]Department of Civil and Environmental Engineering, Environmental Engineering and Water Resources Program, Princeton University, Princeton, NJ, USA

**Abstract.** The influence of the deadtime correction on raindrop size distribution parameters inferred from Joss-Waldvogel disdrometer observations is investigated. The parameters are estimated using a procedure to adjust self-consistent analytical parameterizations to normalized empirical raindrop size distributions. A case study for a squall line system passing over the Goodwin Creek experimental watershed in northern Mississippi (USA) is presented. The data consist of a 2.5-hour time series of one-minute raindrop size distributions collected with a Joss-Waldvogel disdrometer. Application of the deadtime correction increased the estimated rainfall accumulation for the event by almost 15% ($\sim$35 mm before vs. $\sim$40 mm after correction), mainly due to a nearly 35% increase of the peak rain rate during the convective phase of the squall line ($\sim$140 mm h$^{-1}$ before vs. $\sim$190 mm h$^{-1}$ after correction). The exponents of the $Z - R$ relationships inferred using the normalization procedure show a slight decrease for all storm phases (convection, transition, stratiform), whereas the corresponding prefactors increase for all but the transition phase (where the prefactor decreases slightly).

## 1 Introduction

Several approaches towards normalizing raindrop size distributions have been proposed in the scientific literature (e.g. Sekhon and Srivastava, 1971; Willis, 1984; Willis and Tattelman, 1989; Sempere Torres et al., 1994, 1998; Testud et al., 2001; Illingworth and Blackman, 2002). The aim of normalizing (or "scaling") raindrop size distributions is to collapse many individual and highly variable empirical distributions into (ideally) one single "general" (or "intrinsic") distribution, which is typical for a particular type of rain or climatic setting. This provides a statistically more robust manner to adjust analytical parameterizations to raindrop size distributions than the traditional approach where a particular parametric form is fitted to each empirical distribution separately (e.g. Tokay and Short, 1996). An additional advantage of normalizing raindrop size distributions is that it becomes easier to establish connections between the shape of raindrop size distributions and the physical processes producing them (Sempere Torres et al., 2000; Uijlenhoet et al., 2002a, b). This will ultimately lead to improved rainfall retrieval algorithms for ground-based and space-borne microwave remote sensors (both active and passive).

In this paper, we focus on a scaling law formalism for describing raindrop size distributions proposed by Sempere Torres et al. (1994, 1998) and extended by Uijlenhoet (1999). Many previously proposed parameterizations for the raindrop size distribution are special cases of this formulation, notably that of Marshall and Palmer (1948). The advantages of the scaling approach as compared to the previously mentioned normalization procedures are:

1. No a priori assumption is made with regard to the specific parametric form of the scaled spectrum (such as exponential, gamma, lognormal, etc.) – the form follows from the data itself, after the normalization has been applied;

2. It naturally leads to the ubiquitous power law relationships between rainfall integral variables (such as that between the radar reflectivity factor $Z$ and the rain rate $R$);

3. It explicitly considers the issue of the internal consistency of raindrop size distribution parameterizations (e.g. Uijlenhoet and Stricker, 1999; Uijlenhoet, 2001).

We investigate the influence of the deadtime correction (e.g. Waldvogel, 1975; Sauvageot and Lacaux, 1995) on the parameters of the scaled spectra and the associated coefficients of $Z - R$ relationships inferred from Joss-Waldvogel disdrometer observations. Although our investigation is limited to the case of a gamma parameterization for the scaled distribution (comprising the exponential distribution as a special case), the scaling law formalism is able to cope with any desired parametric form.

*Correspondence to:* R. Uijlenhoet
(remko.uijlenhoet@wur.nl)

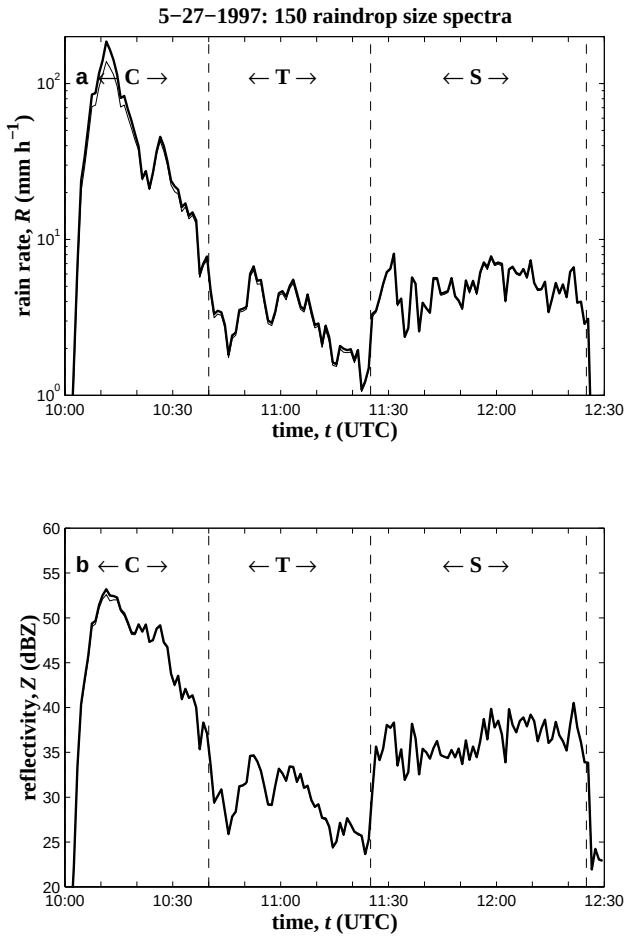


**Fig. 1.** Temporal evolution of (a) rain rate and (b) radar reflectivity factor during three phases of 27 May 1997 squall line, derived from one-minute Joss-Waldvogel disdrometer observations at Goodwin Creek climate station (bold: with deadtime correction; thin: without deadtime correction). 'C', 'T', and 'S' indicate convective, transition, and stratiform phases, respectively, dashed vertical lines their boundaries (10:40 UTC, 11:25 UTC, and 12:25 UTC).

A case study is presented for Joss-Waldvogel disdrometer observations of a squall line passing over a small watershed in northern Mississippi (USA). Because of its particular mesoscale structure, consisting of three different regions with distinctly different microphysical regimes, namely initial convection, transition, and trailing stratiform precipitation (Houze, 1977, 1997; Maki et al., 2001; Bringi et al., 2002), the squall line represents an ideal model for analyzing the variability of raindrop size distributions and associated uncertainties in radar rainfall retrieval algorithms. Analyses of the same squall line event have been presented by Steiner et al. (1999) and Uijlenhoet et al. (2002b). This paper provides an extension of the latter through investigating the influence of the disdrometer deadtime correction on the inferred parameters of the scaled spectra and the associated coefficients of $Z - R$ relationships.

## 2 Methodology

### 2.1 Data

The data selected for our analysis consist of a 2.5-hour time series of one-minute raindrop size distributions collected with a Joss-Waldvogel disdrometer (Joss and Waldvogel, 1967) during a squall line that passed over the Goodwin Creek experimental watershed (Steiner et al., 1999; Alonso and Bingner, 2000) in northern Mississippi on 27 May 1997. The disdrometer is located at the climate station in the center of the 21.4 km$^2$ watershed. The total rainfall accumulation for the event as derived from the disdrometer observations (corrected for the deadtime problem to be discussed in Sect. 3) exceeds 40 mm (32.5 mm during the leading convective line, 2.5 mm during the transition zone, and 5.1 mm during the trailing stratiform rainfall) and the peak rain rate associated with the leading convective line approaches 190 mm h$^{-1}$. Figure 1 shows the time traces of rain rate and radar reflectivity as derived from the disdrometer observations during the event. We only consider spectra associated with rain rates exceeding 1 mm h$^{-1}$. Additional details concerning the measurement process and the associated data analysis are provided by Steiner et al. (1999), Steiner and Smith (2000), and Uijlenhoet et al. (2002b).

### 2.2 Scaling law formalism

According to the scaling law formalism (Sempere Torres et al., 1994, 1998), raindrop size distributions depend both on the raindrop diameter ($D$) and on the value of a so-called reference variable (commonly taken to be the rain rate $R$), following the parametric form

$$N_V(D,R) = R^{\alpha} g(R^{-\beta} D)\,, \tag{1}$$

where: $N_V(D,R)$ (mm$^{-1}$ m$^{-3}$) is the raindrop size distribution as a function of rain rate $R$ (mm h$^{-1}$), i.e. $N_V(D,R)dD$ (m$^{-3}$) is the mean (expected) number of raindrops with (equivalent spherical) diameters between $D$ and $D + dD$ (mm) present per unit volume of air; $\alpha$ and $\beta$ are (dimensionless) *scaling exponents*; and $g(x)$ is the *general raindrop size distribution* as a function of scaled raindrop diameter $x = R^{-\beta} D$, representing the *equivalent* (i.e. scaled) raindrop size distribution at a rain rate of 1 mm h$^{-1}$ (Uijlenhoet, 1999). The values of the scaling exponents indicate whether it is the variability of the raindrop sizes or the variability of the raindrop concentration (or some combination thereof) which controls the variability of the raindrop size distribution. In general, the closer $\beta$ is to zero, the more pronounced is the relative contribution of number-controlled variability (Uijlenhoet, 1999; Uijlenhoet et al., 2002a).

The radar reflectivity factor $Z$ (mm$^6$ m$^{-3}$) is related to the size distribution of the raindrops in the radar sample volume according to

$$Z = \int_0^{\infty} D^6 N_V(D,R) dD \tag{2}$$

(e.g. Battan, 1973). Substituting the scaling law for the raindrop size distribution (Eq. 1) into Eq. (2) leads to the power law

$$Z = aR^b, \tag{3}$$

with

$$a = \int_0^\infty x^6 g(x) dx\,, \tag{4}$$

and

$$b = \alpha + 7\beta \tag{5}$$

(Uijlenhoet, 1999, 2001). Hence, the *prefactor* of a power law $Z - R$ relationship is entirely determined by the shape of the general raindrop size distribution (its 6th moment), whereas a linear combination of the values of the scaling exponents completely determines the exponent of such a power law $Z - R$ relationship.

The rain rate $R$ (in mm h$^{-1}$) is defined in terms of the raindrop size distribution according to

$$R = 6\pi \times 10^{-4} \int_0^\infty D^3 v(D) N_V(D,R) dD\,, \tag{6}$$

where $v(D)$ represents the functional relationship between the raindrop terminal fall speed in still air $v$ (m s$^{-1}$) and the equivalent spherical raindrop diameter $D$ (mm). The only functional form for $v(D)$ that is consistent with power law relationships between rainfall-related variables is the power law

$$v(D) = cD^\gamma\,. \tag{7}$$

(Sempere Torres et al., 1994; Uijlenhoet, 1999, 2001). Typical values for the coefficients of this relationship are $c = 3.778$ (if $v$ is expressed in m s$^{-1}$ and $D$ in mm) and $\gamma = 0.67$ (Atlas and Ulbrich, 1977).

Substituting Eqs. (1) and (7) into the definition of $R$ in terms of the raindrop size distribution (Eq. 6) leads to the *self-consistency constraints*

$$6\pi \times 10^{-4} c \int_0^\infty x^{3+\gamma} g(x) dx = 1 \tag{8}$$

and

$$\alpha + (4+\gamma)\beta = 1 \tag{9}$$

(Sempere Torres et al., 1994). Hence, $g(x)$ must satisfy an integral equation (which reduces its degrees of freedom by one) and there is only one free scaling exponent. These self-consistency constraints guarantee that substitution of the parameterization for the raindrop size distribution (Eq. 1) into the defining expression for $R$ (Eq. 6), leads to $R = R$.

It follows from Eq. (1) that, once the values of $\alpha$ and $\beta$ have been estimated, the shape of $g(x)$ can be identified graphically by plotting scaled versions of the empirical raindrop size distributions $R^{-\alpha} N_V(D,R)$ versus the corresponding scaled raindrop diameters $x = R^{-\beta} D$ (Sempere Torres et al., 1994, 1998; Uijlenhoet, 1999). For the purpose of this paper, consider a gamma parameterization for the general raindrop size distribution,

$$g(x) = \kappa x^\mu \exp(-\lambda x)\,, \tag{10}$$

which for $\mu = 0$ reduces to an exponential parameterization. Substitution of Eq. (10) into (8) yields, for a given value of the parameter $\mu$, a power law relationship of $\kappa$ in terms of $\lambda$,

$$\kappa = \left[6\pi \times 10^{-4} c \Gamma(4+\gamma+\mu)\right]^{-1} \lambda^{4+\gamma+\mu}\,. \tag{11}$$

This is an explicit form of the self-consistency constraint on $g(x)$ for the case of a gamma parameterization. For the applied units, with $c = 3.778$ and $\gamma = 0.67$, Eq. (11) reduces to $\kappa = 9.50\lambda^{4.67}$ for the special case of an exponential parameterization for $g(x)(\mu = 0)$. Substituting Eq. (10) into (1) yields

$$N_V(D,R) = \kappa R^{\alpha-\mu\beta} D^\mu \exp(-\lambda R^{-\beta} D)\,. \tag{12}$$

Equation (12) reduces to the classical gamma parameterization for the raindrop size distribution,

$$N_V(D) = N_0 D^\mu \exp(-\Lambda D) \tag{13}$$

(Ulbrich, 1983), if $N_0$ and $\Lambda$ depend on $R$ according to the power laws

$$N_0 = \kappa R^{\alpha-\mu\beta} \tag{14}$$

and

$$\Lambda = \lambda R^{-\beta}\,. \tag{15}$$

For the special case of an exponential parameterization for the raindrop size distribution of the form initially proposed by Marshall and Palmer (1948), i.e. Eq. (13) with $\mu = 0$, Eq. (14) reduces to $N_0 = \kappa R^\alpha$. Recall that the self-consistency of Eq. (12) requires that $\alpha$ and $\beta$ be related to each other via Eq. (9), and $\kappa$ and $\lambda$ via Eq. (11).

Sempere Torres et al. (1994) have demonstrated that the scaling exponents $\alpha$ and $\beta$ may be estimated as the intercept and slope of a plot of the exponents $\gamma_m$ (of power laws between the moments of order $m$ and $R$) versus the order of the moment $m + 1$. To reduce the effect of instrumental (sampling) effects inherent in disdrometer measurements (e.g. Joss and Waldvogel, 1969), the values of the scaling exponents are estimated using moment orders between two and six ($2 \leq m \leq 6$). To guarantee self-consistency, only $\beta$ is estimated in this manner. The constraint on the scaling exponents (Eq. 9) is subsequently invoked to estimate $\alpha$. Finally, we employ a moment method developed by Uijlenhoet (1999) to estimate self-consistent values of the parameters of the scaled raindrop size distribution $g(x)$. Effectively, this method uses the moments of orders $4 + \gamma$ and $5 + \gamma$ (with $\gamma = 0.67$) of $g(x)$ to estimate $\lambda$ and $\mu$. This corresponds closely to the moment orders (i.e. central in the range 0–6) that are commonly used to estimate the parameters of the gamma raindrop size distribution (e.g. Tokay and Short, 1996; Ulbrich and Atlas, 1998). The corresponding self-consistent value of $\kappa$ is subsequently estimated using Eq. (11).

**Table 1.** Rainfall accumulations and maximum rain rates for three phases of 27 May 1997 squall line and for entire event estimated with and without deadtime correction

| Storm phase | Rainfall accumulation (mm) | | Maximum rainrate (mm $h^{-1}$) | |
|---|---|---|---|---|
| | With correction | Without correction | With correction | Without correction |
| Convective | 32.5 | 27.7 | 186.3 | 138.6 |
| Transition | 2.5 | 2.4 | 6.7 | 6.4 |
| Stratiform | 5.1 | 5.0 | 8.1 | 7.9 |
| Total | 40.1 | 35.1 | 186.3 | 138.6 |

## 3 Results and discussion

Observations with the Joss-Waldvogel disdrometer are prone to the so-called deadtime problem. This instrumental effect is associated with a resonance ('ringing') of the styrofoam cone of the disdrometer following the impact of a large drop. This causes such a strong internal noise response that the signal due to any small drop arriving during the ensuing few milliseconds – the 'deadtime' – is not detectable (e.g. Waldvogel, 1975; Sauvageot and Lacaux, 1995). Applying the deadtime correction proposed by the manufacturer of the instrument (Distromet Ltd., Switzerland) has the effect of increasing the numbers of small raindrops, mainly in those empirical spectra where many large drops are present, i.e. at high rain rates. Higher order moments of the raindrop size distribution (such as rain rate and radar reflectivity), which are less dependent on the numbers of small drops, are going to be less affected than lower order moments (such as drop concentration, mean diameter, and diameter standard deviation). The correction is not perfect, however, because due to its multiplicative nature it is not able to create drops in bins where none have been detected.

Figure 1 shows that the effect of the deadtime correction on rain rate and radar reflectivity is only appreciable for the most intense part of the squall line (between 10:10 and 10:20 UTC). This is confirmed by Table 1, which quantifies the effect of the deadtime correction on the rainfall accumulations and maximum rain rates during the three phases of the storm. Figure 2 shows the effect of the deadtime correction on the time traces of raindrop concentration, mean diameter, and diameter standard deviation. Application of the deadtime correction leads to a doubling of the raindrop concentrations during the convective phase of the squall line, while the effect remains appreciable during the transition and stratiform phases (Fig. 2a). The net effect of the increased numbers of small drops produced by the deadtime correction is to decrease the mean raindrop diameter, mainly during the most intense part of the storm (Fig. 2b). The standard deviation of the raindrop diameters is not as strongly affected by the deadtime correction, although it displays a slight decrease during the convective and stratiform phases of the squall line (Fig. 2c).

In Fig. 3a the exponents $\gamma_m$ of power law relationships between the $m$th order moment of the empirical raindrop

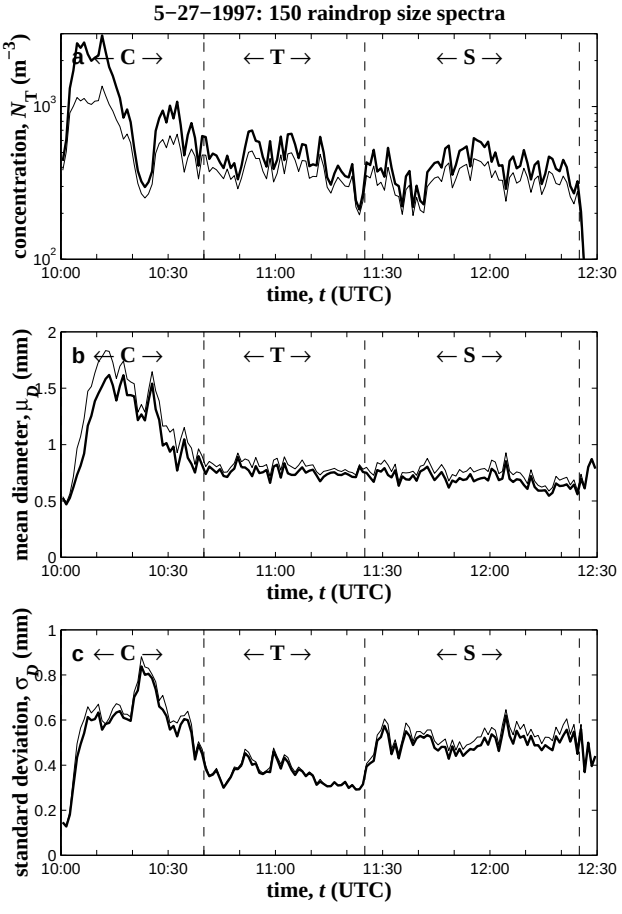


**Fig. 2.** Temporal evolution of (a) raindrop concentration, (b) mean raindrop diameter, and (c) standard deviation of raindrop diameters during three phases of 27 May 1997 squall line, derived from one-minute Joss-Waldvogel disdrometer observations (bold: with deadtime correction; thin: without deadtime correction).

size distributions (for $0 \leq m \leq 6$) and the reference variable $R$ are plotted against the corresponding moment orders $m+1$ for the 38 convective spectra considered. As opposed to the analysis for the same event presented by Uijlenhoet et al. (2002b), the disdrometer deadtime correction (Waldvogel, 1975; Sauvageot and Lacaux, 1995) has been applied here. The power law relationships have been adjusted using linear regression on the logarithmic values, using $\log R$ as

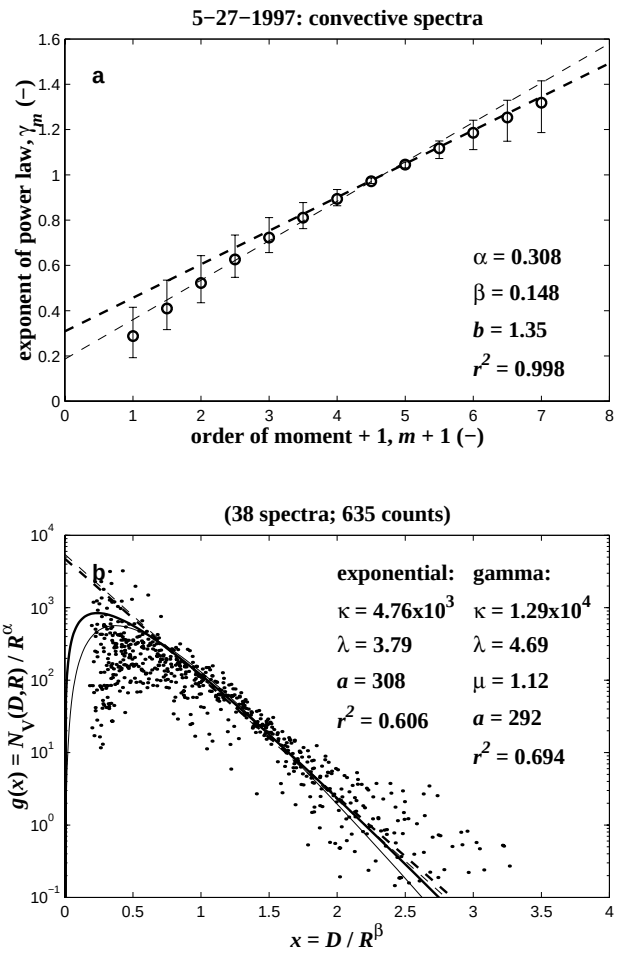


**Fig. 3.** Scaling analysis of raindrop size distributions (with deadtime correction) collected during convective phase of 27 May 1997 squall line. (a) Estimation of scaling exponents $(\alpha, \beta)$ as intercept and slope of plot of exponents $\gamma_m$ (of power laws with $R$) vs. order of moment $m + 1$ for $m \geq 2$ (error bars indicate 68% confidence limits obtained using 1000 bootstrap samples). Corresponding values of exponent $b$ $(-)$ of $Z - R$ relationship and of coefficient of determination $r^2$ $(-)$ of regression line (bold: with deadtime correction; thin: without deadtime correction) are indicated as well. (b) Application of exponents to scale spectra and infer general raindrop size distribution (dots) and adjustment of theoretical parameterizations for $g(x)$ (bold: with deadtime correction; thin: without deadtime correction), with corresponding parameter values, prefactors $a$ $(-)$ of $Z - R$ relationships, and coefficients of determination $r^2$ $(-)$: exponential parameterization (dashed line) and gamma parameterization (solid line).

the independent variable. The error bars indicate 68% confidence limits, estimated from 1000 bootstrap samples (Efron and Tibshirani, 1993). According to the scaling law theory (Sempere Torres et al., 1994), a plot like Fig. 3a should yield a straight line with intercept $\alpha$ and slope $\beta$. The bold dashed line indicates a linear regression between $\gamma_m$ and $m + 1$ for $2 \leq m \leq 6$. The straight-line behavior predicted by the scaling law formalism holds reasonably well over a large part of the range of moment orders from 0 to 6. This is confirmed by the high value of the coefficient of determination $r^2$ (computed as the square of the correlation coefficient between $\gamma_m$ and $m + 1$ for $2 \leq m \leq 6$). As explained in Sect. 2, in order to guarantee self-consistency, the value of $\beta$ has been determined as the slope of the dashed line in Fig. 3a and the value of $\alpha$ from the self-consistency constraint on the scaling exponents (Eq. 9), although the difference with the intercept of the dashed line is small. The indicated value of $b$ is the exponent of the corresponding $Z - R$ relationship implied by the scaling law formalism (Eq. 5).

For comparison, the resulting linear regression without disdrometer deadtime correction has been plotted in Fig. 3a as well (thin dashed line). Apparently, the effect of applying the deadtime correction on the scaling exponents is to increase the value of $\alpha$ (the intercept of the regression line) and to decrease the value of $\beta$ (its slope). The net result is a slight decrease of the inferred value of the $Z - R$ exponent $b$ (Table 2). The result of applying the correction is that lower order moments (which depend stronger on the numbers of small drops than higher order moments) are increased at higher rain rates, whereas they remain largely unaffected at lower rain rates (when less large drops are present). The net effect is that the exponents of power law relationships between lower order moments and rain rate tend to get increased, which is exactly what we observe (Fig. 3a).

In Fig. 3b the inferred values for the scaling exponents are used to identify the shape of the corresponding general raindrop size distribution $g(x)$. The scaling analysis is successful in the sense that it eliminates a large part of the rain rate-induced variability, as predicted by the scaling law formalism. The fact that not all dots fall perfectly on one single curve indicates that one reference variable (in this case the rain rate $R$) is apparently not able to explain all observed variability. Two different analytical parameterizations have been fitted to the empirical general raindrop size distribution indicated by the dots: an exponential parameterization (bold dashed line) and a gamma parameterization (bold solid line). Equations (10) and (11) explain the meaning of the parameter values indicated in Fig. 3b (recall that $\mu = 0$ for the exponential parameterization). The indicated values of $a$ are the values for the prefactors of the corresponding $Z - R$ relationships implied by the scaling law formalism for the two parameterizations (Eq. 4). Also shown are the corresponding values of the *coefficient of determination* (or *model efficiency*) $r^2$ $(-)$, which indicates the fraction of the observed variance explained by the model. For comparison, the resulting curve-fits *without* disdrometer deadtime correction have been plotted in Fig. 3b as well (thin lines), although it should be noted that the data points plotted in Fig. 3b are those *with* deadtime correction. The effect of applying the deadtime correction on the exponential adjustment to the empirical $g(x)$ is hardly discernable, whereas the gamma fit reflects a slight increase in the numbers of small drops associated with the correction. The net result is an increase of the inferred values of the $Z - R$ prefactor $a$, both for the exponential and for the gamma fit (Table 2).

Similar scaling analyses have been carried out for the tran-

**Table 2.** Inferred values (with and without deadtime correction) of the following parameters for convective, transition, and stratiform phases of 27 May 1997 squall line: scaling exponents ($\alpha, \beta$) and corresponding exponent $b$ of $Z - R$ relationship; intercept $\kappa$, (semi-logarithmic) slope $\lambda$ of exponential fit to general raindrop size distribution $g(x)$, and corresponding prefactor $a$ of $Z - R$ relationship; parameters $\kappa$, $\lambda$, and $\mu$ of gamma parameterization for general raindrop size distribution $g(x)$, and corresponding prefactor $a$ of $Z - R$ relationship

| Convective phase (38 spectra) | | | |
|---|---|---|---|
| | Parameter | With correction | Without correction |
| General | $\alpha$ | 0.308 | 0.186 |
| | $\beta$ | 0.148 | 0.174 |
| | $b$ | 1.35 | 1.41 |
| Exponential | $\kappa$ | $4.76\times10^3$ | $5.47\times10^3$ |
| | $\lambda$ | 3.79 | 3.90 |
| | $a$ | 308 | 287 |
| Gamma | $\kappa$ | $1.29\times10^4$ | $3.73\times10^4$ |
| | $\lambda$ | 4.69 | 5.66 |
| | $\mu$ | 1.12 | 2.11 |
| | $a$ | 292 | 264 |
| Transition phase (45 spectra) | | | |
| | Parameter | With correction | Without correction |
| General | $\alpha$ | – 0.006 | – 0.061 |
| | $\beta$ | 0.215 | 0.227 |
| | $b$ | 1.50 | 1.53 |
| Exponential | $\kappa$ | $1.28\times10^4$ | $1.19\times10^4$ |
| | $\lambda$ | 4.68 | 4.61 |
| | $a$ | 188 | 195 |
| Gamma | $\kappa$ | $1.43\times10^6$ | $2.40\times10^6$ |
| | $\lambda$ | 9.06 | 9.54 |
| | $\mu$ | 4.37 | 5.00 |
| | $a$ | 164 | 169 |
| Stratiform phase (60 spectra) | | | |
| | Parameter | With correction | Without correction |
| General | $\alpha$ | 0.281 | 0.199 |
| | $\beta$ | 0.154 | 0.171 |
| | $b$ | 1.36 | 1.40 |
| Exponential | $\kappa$ | $1.98\times10^3$ | $2.09\times10^3$ |
| | $\lambda$ | 3.14 | 3.17 |
| | $a$ | 476 | 464 |
| Gamma | $\kappa$ | $6.84\times10^3$ | $9.67\times10^3$ |
| | $\lambda$ | 4.33 | 4.65 |
| | $\mu$ | 1.78 | 2.17 |
| | $a$ | 442 | 425 |

sition (Fig. 4) and the stratiform (Fig. 5) phases of the squall line system. These analyses reveal that the shapes of the scaled spectra are wide and bent downward for small raindrop sizes in the leading convective line, narrow and slightly bent upward in the transition zone, and wide and strongly bent upward in the trailing stratiform rain. The dispersion among the scaled spectra during the transition and stratiform phases is significantly smaller than during the convective phase. The exponents ($b$) of the resulting $Z - R$ relationships are roughly the same for the leading convective line and the trailing stratiform rain ($\approx 1.4$) and slightly larger for the transition region ($\approx 1.5$), with prefactors ($a$) increasing in the order transition ($\approx 200$), convective ($\approx 300$), stratiform ($\approx 450$). The effect of the deadtime correction on the $Z - R$ relationships inferred using the scaling law formalism is a slight decrease of the exponents for all storm phases and an increase of the prefactors for all but the transition phase (where the $Z - R$ prefactor decreases slightly). Table 2 summarizes the inferred parameter values.

Figure 6 shows in detail the effect of the deadtime correction on the inferred values of the scaled raindrop diameter $x = D/R^\beta$ and the corresponding values of the general raindrop size distribution function $g(x) = N_V(D, R)/R^\alpha$ for each of the three phases of the squall line. The net effect of the deadtime correction on $x$ is the combined result of higher values of $R$ (which tends to decrease $x$) and a lower value of $\beta$ (which tends to increase $x$ if $R > 1$ mm h$^{-1}$). Figure 6 shows that the data points ('plus'-signs), particularly during the convective and stratiform phases of the storm (top left-hand and bottom left-hand panels, respectively), are located *above* the diagonal line indicating 1:1 correspondence between the uncorrected ('raw') and corrected values of $x$. Hence, application of the deadtime correction leads to increased values of the scaled raindrop diameter $x$. Apparently,

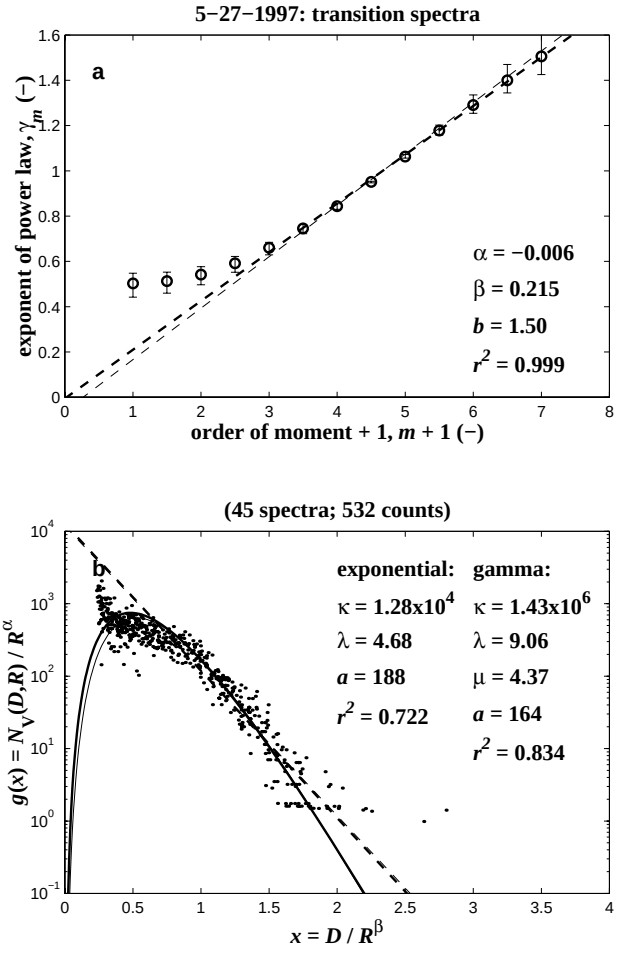


**Fig. 4.** Same as Fig. 3 for raindrop size distributions collected during transition phase of 27 May 1997 squall line.

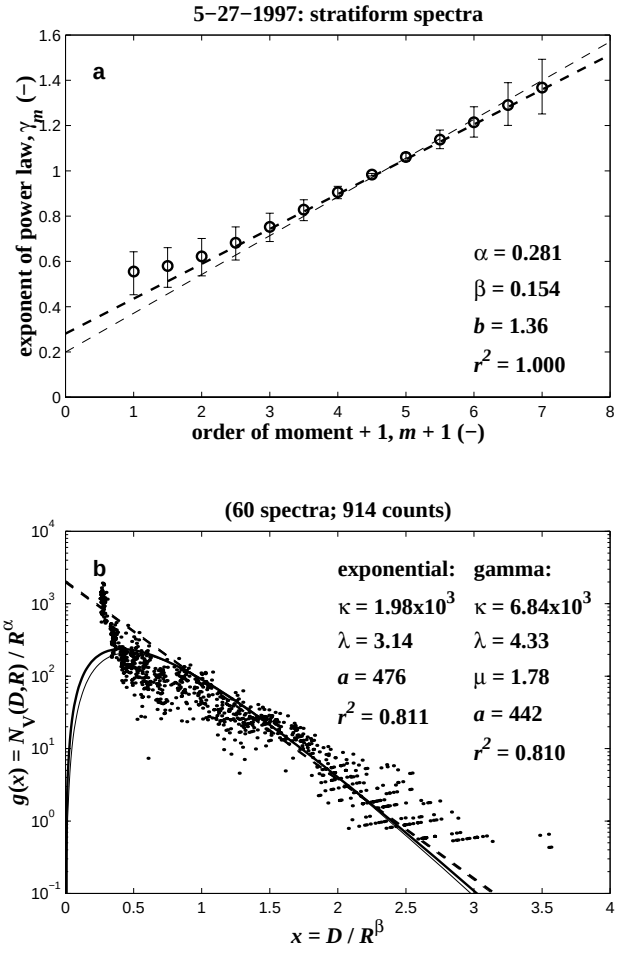


**Fig. 5.** Same as Fig. 3 for raindrop size distributions collected during stratiform phase of 27 May 1997 squall line.

the influence of $\beta$ on $x$ is stronger than that of $R$.

The net effect of the deadtime correction on $g(x)$ is the combined result of higher values of $N_V(D,R)$ (which tends to increase $g(x)$), higher values of $R$ (which tends to decrease $g(x)$), and a higher value of $\alpha$ (which tends to decrease $g(x)$ if $R > 1$ mm h$^{-1}$). Figure 6 shows that lower values of $g(x)$ (corresponding to the tails of the distributions, where the effect of increased $N_V(D,R)$ is negligible) are decreased, whereas higher values of $g(x)$ (corresponding to the small-size end of the spectra, where the effect of increased $N_V(D,R)$ dominates) are increased, particularly during the convective phase of the storm (top right-hand panel).

## 4 Conclusions

This work provides an extension of that presented by Uijlenhoet et al. (2002b). Its main conclusions can be summarized as follows:

1. A procedure to adjust self-consistent analytical parameterizations to normalized empirical raindrop size distributions has been successfully applied to a 2.5-hour time series of Joss-Waldvogel disdrometer data for a squall line system passing over the Goodwin Creek experimental watershed in northern Mississippi (USA).

2. Application of the deadtime correction increased the estimated rainfall accumulation for the event by almost 15% (∼35 mm before vs. ∼40 mm after correction), mainly due to a nearly 35% increase of the peak rain rate during the convective phase of the squall line (∼140 mm h$^{-1}$ before vs. ∼190 mm h$^{-1}$ after correction).

3. Application of the deadtime correction lead to a strong increase of the raindrop concentrations, an appreciable decrease of the mean raindrop diameters, and a slight decrease of the standard deviations of the raindrop diameters. The radar reflectivity factor was hardly affected.

4. The effect of applying the deadtime correction on the $Z - R$ relationships inferred using the developed normalization procedure showed a slight decrease of the exponents for all storm phases and an increase of the

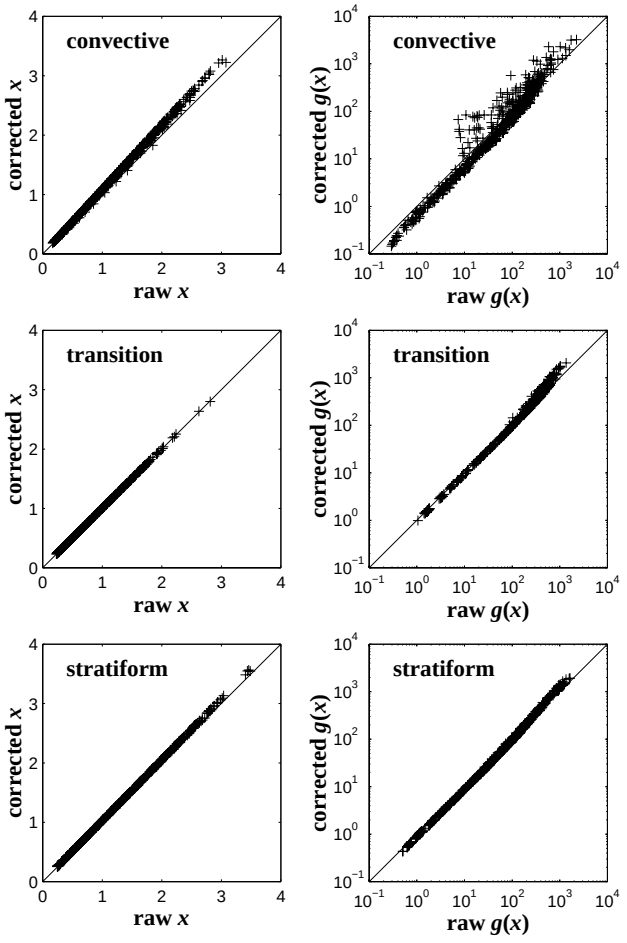


**Fig. 6.** Comparison of scaled raindrop diameters $x$ and corresponding values of general raindrop size distribution $g(x)$ with ('corrected') and without deadtime correction ('raw') for three phases of 27 May 1997 squall line, derived from one-minute Joss-Waldvogel disdrometer observations (diagonal lines indicate 1:1 correspondence between uncorrected and corrected values).

prefactors for all but the transition phase (where the $Z - R$ prefactor decreased slightly).

*Acknowledgement.* The extraordinary assistance of the staff of the USDA/ARS National Sedimentation Laboratory in Oxford, Mississippi, in maintaining and operating the disdrometer is greatly appreciated. This work was supported by National Science Foundation grants EAR-9909696 and ATM-9906012, the National Weather Service and the NEXRAD Operations Support Facility under Cooperative Agreement NA87WH0518, National Aeronautics and Space Administration grant NAG5-7744, and United States Army Research Office grant DAAD19-99-1-0163. The lead author is supported by the Netherlands Organization for Scientific Research (NWO), through grant 016.021.003 in the framework of the Innovational Research Incentives Scheme (Vernieuwingsimpuls).

## References

Alonso, C. V., and R. L. Bingner, 2000: Goodwin Creek Experimental Watershed: A unique field laboratory. ASCE J. Hydraul. Eng., 126, 174-177.

Atlas, D., and C. W. Ulbrich, 1977: Path- and area integrated rainfall measurement by microwave attenuation in the 1-3 cm band. J. Appl. Meteor., 16, 1322-1331.

Battan, L. J., 1973: Radar Observation of the Atmosphere. The University of Chicago Press, 324 pp.

Bringi, V. N., G.-J. Huang, V. Chandrasekar, and E. Gorgucci, 2002: A methodology for estimating the parameters of a gamma raindrop size distribution model from polarimetric radar data: Application to a squall-line event from the TRMM/Brazil campaign. J. Atmos. Oceanic Technol., 19, 633-645.

Efron, B., and R. Tibshirani, 1993: An Introduction to the Bootstrap. Chapman and Hall, 436 pp.

Houze, R. A., Jr., 1977: Structure and dynamics of tropical squall-line system. Mon. Wea. Rev., 105, 1540–1567.

Houze, R. A., Jr., 1997: Stratiform precipitation in regions of convection: A meteorological paradox? Bull. Amer. Meteor. Soc., 78, 2179-2196.

Illingworth, A. J., and T. M. Blackman, 2002: The need to represent raindrop size spectra as normalized gamma distributions for the interpretation of polarization radar observations. J. Appl. Meteor., 41, 286-297.

Joss, J., and A. Waldvogel, 1967: Ein Spektrograph für Niederschlagstropfen mit automatischer Auswertung. Pure Appl. Geophys., 68, 240-246.

Joss, J., and A. Waldvogel, 1969: Raindrop size distribution and sampling size errors. J. Atmos. Sci., 26, 566-569.

Maki, M., T. D. Keenan, Y. Sasaki, and K. Nakamura, 2001: Characteristics of the raindrop size distribution in tropical continental squall lines observed in Darwin, Australia. J. Appl. Meteor., 40, 1393-1412.

Marshall, J. S., and W. McK. Palmer, 1948: The distribution of raindrops with size. J. Meteor., 5, 165-166.

Sauvageot, H., and J.-P. Lacaux, 1995: The shape of averaged raindrop size distributions. J. Atmos. Sci., 52, 1070-1083.

Sekhon, R. S., and R. C. Srivastava, 1971: Doppler radar observations of drop-size distributions in a thunderstorm. J. Atmos. Sci., 28, 983-994.

Sempere Torres, D., J. M. Porrà, and J.-D. Creutin, 1994: A general formulation for raindrop size distribution. J. Appl. Meteor., 33, 1494-1502.

Sempere Torres, D., J. M. Porrà, and J.-D. Creutin, 1998: Experimental evidence of a general description of raindrop size distribution properties. J. Geophys. Res. (D), 103, 1785-1797.

Sempere Torres, D., R. Sánchez-Diezma, I. Zawadzki, and J.-D. Creutin, 2000: Identification of stratiform and convective areas using radar data with application to the improvement of DSD analysis and $Z - R$ relations. Phys. Chem. Earth, 25, 985-990.

Steiner, M., and J. A. Smith, 2000: Reflectivity, rain rate, and kinetic energy flux relationships based on raindrop spectra. J. Appl. Meteor., 39, 1923-1940.

Steiner, M., J. A. Smith, S. J. Burgess, C. V. Alonso, and R. W. Darden, 1999: Effect of bias adjustment and rain gauge data quality control on radar rainfall estimation. Water Resour. Res., 35, 2487-2503.

Testud, J., S. Oury, R. A. Black, P. Amayenc, and X. Dou, 2001: The concept of "normalized" distribution to describe raindrop spectra: A tool for cloud physics and cloud remote sensing. J. Appl. Meteor., 40, 1118-1140.

Tokay, A., and D. A. Short, 1996: Evidence from tropical raindrop spectra of the origin of rain from stratiform versus convective clouds. J. Appl. Meteor., 35, 355-371.

Uijlenhoet, R., 1999: Parameterization of Rainfall Microstructure for Radar Meteorology and Hydrology. Doctoral dissertation, Wageningen University, the Netherlands, 279 pp. (available from the author).

Uijlenhoet, R., 2001: Raindrop size distributions and radar reflectivity-rain rate relationships for radar hydrology. Hydrol. Earth Syst. Sci., 5, 615-627.

Uijlenhoet, R., and J. N. M. Stricker, 1999: A consistent rainfall parameterization based on the exponential raindrop size distribution. J. Hydrol., 218, 101-127.

Uijlenhoet, R., J. A. Smith, and M. Steiner, 2002a: The microphysical structure of extreme precipitation as inferred from ground-based raindrop size spectra, (conditionally accepted for publication in J. Atmos. Sci.).

Uijlenhoet, R., M. Steiner, and J. A. Smith, 2002b: Variability of raindrop size distributions in a squall line and implications for radar rainfall estimation (accepted for publication in J. Hydrometeor.).

Ulbrich, C. W., 1983: Natural variations in the analytical form of the raindrop size distribution. J. Clim. Appl. Meteor., 22, 1764-1775.

Ulbrich, C. W., and D. Atlas, 1998: Rainfall microphysics and radar properties: Analysis methods for drop size spectra. J. Appl. Meteor., 37, 912-923.

Waldvogel, A., 1975: Acoustic noise correction for the disdrometer. Internal Report, Laboratory for Atmospheric Physics, Swiss Federal Institute of Technology, 8 pp.

Willis, P. T., 1984: Functional fits to some observed drop size distributions and parameterization of rain. J. Atmos. Sci., 41, 1648-1661.

Willis, P. T., and P. Tattelman, 1989: Drop-size distributions associated with intense rainfall. J. Appl. Meteor., 28, 3-15.